J|A|C|S ARTICLES

Published on Web 03/10/2010

Light-Harvesting Conjugated Microporous Polymers: Rapid and Highly Efficient Flow of Light Energy with a Porous Polyphenylene Framework as Antenna

Long Chen,[†] Yoshihito Honsho,[‡] Shu Seki,[‡,§] and Donglin Jiang*[,†,§]

Department of Materials Molecular Science, Institute for Molecular Science, 5-1 Higashiyama, Myodaiji, Okazaki 444-8787, Japan, Department of Applied Chemistry, Graduate School of Engineering, Osaka University, 2-1 Yamadaoka, Suita, Osaka 565-0871, Japan, and PRESTO, JST, Japan

Received January 13, 2010; E-mail: jiang@ims.ac.jp

Abstract: The molecular design of light-harvesting antennae requires not only the segregation of a large number of chromophore units in a confined nanospace but also the cooperation of these units in achieving highly efficient energy transduction. This article describes the synthesis and functions of a polyphenylene-based conjugated microporous polymer (PP-CMP). PP-CMP was recently designed and synthesized by Suzuki polycondensation reaction and used as an antenna for the noncovalent construction of a light-harvesting system. In contrast to linear polyphenylene, PP-CMP consists of conjugated three-dimensional polyphenylene scaffolds and holds inherent porous structure with uniform pore size (1.56 nm) and large surface area (1083 $m^2\ g^{-1}$). It emits blue photoluminescence, is capable of excitation energy migration over the framework, and enables rapid transportation of charge carrier with intrinsic mobility as high as 0.04 $cm^2\ V^{-1}\ s^{-1}$. The microporous structure of PP-CMP allows for the spatial confinement of energy-accepting coumarin 6 molecules in the pores and makes the high-throughput synthesis of light-harvesting systems with designable donor−acceptor compositions possible. Excitation of the PP-CMP skeleton leads to brilliant green emission from coumarin 6, with an intensity 21-fold as high as that upon direct excitation of coumarin 6 itself, while the fluorescence from PP-CMP itself is wholly quenched as a result of energy transfer from the light-harvesting PP-CMP framework to coumarin 6. The PP-CMP skeleton is highly cooperative, with an average of 176 phenylene units working together to channel the excitation energy to one coumarin 6 molecule, and features the energy-transfer process with quick, efficient, and vectorial character. These unique characteristics clearly originate from the conjugated porous structure and demonstrate the usefulness of CMPs in the exploration of π-electronic functions, in addition to their gas adsorption properties thus far reported.

Introduction

Conjugated microporous polymers (CMPs) are a new class of porous materials with an amorphous three-dimensional organic framework.[1−8] Unlike other porous materials, CMPs are unique in that they enable the elaborate integration of π-electronic components to the covalent framework while retaining a permanent porous structure. Most studies on CMPs to date have focused on the development of synthetic approaches for the control of pore size and surface area.[2−6] However, the functions of CMPs, apart from gas storage, have not yet been

[†] Institute for Molecular Science.
[‡] Osaka University.
[§] JST.

(1) (a) Cooper, A. I. *Adv. Mater.* **2009**, *21*, 1291–1295. (b) Thomas, A.; Kuhn, P.; Weber, J.; Titirici, M.-M.; Antonietti, M. *Macromol. Rapid Commun.* **2009**, *30*, 221–236.

(2) (a) Jiang, J. X.; Su, F.; Trewin, A.; Wood, C. D.; Campbell, N. L.; Niu, H.; Dickinson, C.; Ganin, A. Y.; Rosseinsky, M. J.; Khimyak, Y. Z.; Cooper, A. I. *Angew. Chem., Int. Ed.* **2007**, *46*, 8574–8578. (b) Jiang, J. X.; Su, F.; Trewin, A.; Wood, C. D.; Niu, H.; Jones, T. A.; Khimyak, Y. Z.; Cooper, A. I. *J. Am. Chem. Soc.* **2008**, *130*, 7710–7720. (c) Jiang, J. X.; Su, F.; Niu, H.; Wood, C. D.; Campbell, N. L.; Khimyak, Y. Z.; Cooper, A. I. *Chem. Commun.* **2008**, *48*, 6–488. (d) Dawson, R.; Su, F.; Niu, H.; Wood, C. D.; Jones, J. T. A.; Khimyak, Y. Z.; Cooper, A. I. *Macromolecules* **2008**, *41*, 1591–1593. (e) Stöckel, E.; Wu, X.; Trewin, A.; Wood, C. D.; Clowes, R.; Campbell, N. L.; Jones, J. T. A.; Khimyak, Y. Z.; Adams, D. J.; Cooper, A. I. *Chem. Commun.* **2009**, 212–214. (f) Jiang, J. X.; Trewin, A.; Su, F.; Wood, C. D.; Niu, H.; Jones, J. T. A.; Khimyak, Y. Z.; Cooper, A. I. *Macromolecules* **2009**, *42*, 2658–2666. (g) Dawson, R.; Laybourn, A.; Clowes, R.; Khimyak, Y. Z.; Adams, D. J.; Cooper, A. I. *Macromolecules* **2009**, *42*, 8809–8816.

(3) (a) Kuhn, P.; Antonietti, M.; Thomas, A. *Angew. Chem., Int. Ed.* **2008**, *47*, 3450–3453. (b) Kuhn, P.; Forget, A.; Su, D.; Thomas, A.; Antonietti, M. *J. Am. Chem. Soc.* **2008**, *130*, 13333–13337. (c) Kuhn, P.; Thomas, A.; Antonietti, M. *Macromolecules* **2009**, *42*, 319–326. (d) Weber, J.; Thomas, A. *J. Am. Chem. Soc.* **2008**, *130*, 6334–6335. (e) Schmidt, J.; Werner, M.; Thomas, A. *Macromolecules* **2009**, *42*, 4426–4429. (f) Schmidt, J.; Weber, J.; Epping, J. D.; Antonietti, M.; Thomas, A. *Adv. Mater.* **2009**, *21*, 702–705.

(4) (a) Schwab, M. G.; Fassbender, B.; Spiess, H. W.; Thomas, A.; Feng, X.; Müllen, K *J. Am. Chem. Soc.* **2009**, *131*, 7216–7217. (b) Feng, X.; Liang, Y.; Zhi, L.; Thomas, A.; Wu, D.; Lieberwirth, I.; Kolb, U.; Müllen, K. *Adv. Funct. Mater.* **2009**, *19*, 2125–2129.

(5) Farha, O. K.; Spokoyny, A. M.; Hauser, B. G.; Bae, Y.-S.; Brown, S. E.; Snurr, R. Q.; Mirkin, C. A.; Hupp, J. T. *Chem. Mater.* **2009**, *21*, 3033–3035.

(6) Rose, M.; Bohlmann, W.; Sabo, M.; Kaskel, S. *Chem. Commun.* **2008**, *246*, 2–2464.

(7) Zhang, Y.; Riduan, S. N.; Ying, J. Y. *Chem.—Eur. J.* **2009**, *15*, 1077–1081.

(8) Palkovits, R.; Antonietti, M.; Kuhn, P.; Thomas, A.; Schüth, F. *Angew. Chem., Int. Ed.* **2009**, *48*, 6909–6912.

 10.1021/ja100327h

well explored.[3f,7,8] We have focused on the development of photofunctional CMPs with the expectation that the energy-donating CMPs with highly dense π-electronic components could serve as antennae for the collection of photons, while inherent pores within the framework could spatially confine energy-accepting counterparts, thus leading to the creation of an unprecedented donor−acceptor system for energy transduction mediated by the three-dimensional porous framework.

The molecular design of artificial light-harvesting antennae and fabrication of vectorial energy-transferring systems have attracted significant attention, with an aim to mimic natural photosynthetic systems, and have driven the exploration of novel materials for excitation energy and charge carrier transportation. A light-harvesting scaffold requires the incorporation of many light-absorbing units to provide a large absorption cross-section to capture dilute photons. Importantly, the light-absorbing units need to be designed in a way that they are cooperative in triggering the energy-transfer process. Previously, star-shaped, dendritic, and hyperbranched polymers with dense pigment moieties have been synthesized for the capture of photons; few examples of them show the cooperative effect in the excitation energy transfer.[9,10] Nevertheless, the construction of dendritic and well-defined hyperbranched polymeric light-harvesting systems involves tedious synthetic and purification work. Meanwhile, the optimization of donor−acceptor ratios to maximize the light-harvesting capability eventually requires changing the size and structure of the polymers. In sharp contrast, CMPs, owing to their inherent porous structures, allow for the noncovalent confinement of acceptor molecules in the 3D pores, and thus tuning donor−acceptor compositions is straightforward and facile. Therefore, the advantages of CMPs over hyperbranched and dendritic polymers are clear. CMPs constitute permanent pores within a π-electronic framework and allow for high-throughput synthesis of energy transduction systems with designable donor−acceptor compositions via physical confinement, without any change in the polymer structure and composition. Here we report the first example of light-harvesting CMPs with porous polyphenylene scaffold as an antenna and highlight a vectorial, speedy, and highly efficient excitation energy funneling with the newly synthesized PP-CMP (Chart 1).

Experimental Section

1,2,4,5-Tetrabromobenzene (TBB) and 1,4-benzene diboronic acid (BDBA) were obtained from Tokyo Kasei (TCI). Anhydrous organic solvents for reactions, potassium carbonate, and tetrakis(triphenylphosphine)palladium(0) were obtained from Kanto Chemicals. A mixture of TBB (153 mg, 0.39 mmol) and BDBA (129 mg, 0.78 mmol) in dimethylformamide (DMF, 12 mL) was degassed by three freeze−pump−thaw cycles. To the mixture was added an aqueous solution of K_2CO_3 (2.0 M, 1.5 mL) and tetrakis(triphenylphosphine)palladium(0) (45 mg, 39 μmol). The mixture was degassed by three freeze−pump−thaw cycles, purged with Ar, and stirred at 150 °C for 24 h. The mixture was allowed to cool at room temperature and poured into water. The precipitate was collected by filtration, thoroughly washed with water, dichloromethane, and methanol, dried under vacuum at 100 °C, and rigorously washed by Soxhlet extractions for 24 h with water, dichloromethane, methanol, and tetrahydrofuran (THF), respectively, to give PP-CMP (103 mg) as a gray solid in quantitative yield.

Results and Discussion

PP-CMP was synthesized quantitatively by a Suzuki cross-coupling polycondensation reaction[11] with BDBA and TBB as monomers in the presence of Pd(0) as catalyst in an alkaline mixture of DMF/water (for characterization see Supporting Information, Tables S1 and S2, Figure S1). The solid-state $^1H-^{13}C$ CP/MAS NMR spectrum of PP-CMP recorded at a MAS rate of 15 kHz and a CP contact time of 2 ms displayed two broad peaks at 140.2 and 129.0 ppm, corresponding to substituted and unsubstituted phenyl carbons, respectively (Figure 1). Field-emission scanning electron microscopy (FE-SEM) showed that PP-CMP adopts a sphere shape with particle sizes from 50 to 100 nm (Figure 2a). High-resolution transmission electron microscopy (HR TEM) revealed the presence of cavities (Figure 2b). Selected area electron diffration (SAED) measurements did not show any sign of crystallinity (Figure 2b, inset), and the powder X-ray diffraction (PXRD) profile reveals amorphous character (Figure S2). Gas sorption measurements with N_2 at 77 K displayed a typical type-IV sorption isotherm curve, which is suggestive of a microporous structure (Figure 3a). The Brunauer−Emmett−Teller (BET) surface area was evaluated to be 1083 $m^2\ g^{-1}$, and the pore width was calculated by the nonlocal density functional theory (NLDFT) method to be 1.56 nm (Figure 3b). The cumulative pore volume profile indicated a predominance of 1.56 nm width pores in the framework (Figure 3b).

PP-CMP dispersed in CH_2Cl_2/polyethylene glycol (PEG) at 25 °C showed an absorption band at 363 nm, which is close to the absorption maximum (365 nm) for infinitely long one-dimensional polyphenylene.[12,13] Upon excitation at 363 nm, PP-CMP emitted blue luminescence centered at 443 nm with a quantum yield of about 23% (Figure 4a, solid blue curve). The excitation spectrum monitored at 443 nm displayed a peak at 363 nm (dotted blue curve). On the other hand, coumarin 6 in CH_2Cl_2 emitted at 497 nm (Figure 4b, solid green curve), and the excitation spectral profile showed a peak at 458 nm (dotted green curve). In relation to this observation, a control experiment showed that coumarin 6 is hardly emissive upon excitation at 363 nm (Figure 4b, dotted orange curve), which makes the selective excitation of the PP-CMP framework possible. These observations suggest that coumarin 6 could serve as an energy-accepting counterpart for the energy-donating PP-CMP framework, since its absorption band overlaps with the emission band of PP-CMP, which would favor a fluorescence resonance energy transfer. As a typical protocol, PP-CMP powder (10 mg) was degassed under high vacuum and added via syringe with a designated amount of coumarin 6 in degassed ethanol (10 mL),

(9) (a) Mukhopadhyay, P.; Iwashita, Y.; Shirakawa, M.; Kawano, S.; Fujita, N.; Shinkai, S. *Angew. Chem., Int. Ed.* **2006**, *45*, 1592–1595. (b) Jiang, D.-L.; Aida, T. *Nature* **1997**, *388*, 454–456. (c) Jiang, D.-L.; Aida, T. *J. Am. Chem. Soc.* **1998**, *120*, 10895–10901. (d) Saito, T.; Jiang, D.-L.; Aida, T. *J. Am. Chem. Soc.* **1999**, *121*, 10658–10659. (e) Choi, M.-S.; Aida, T.; Yamazaki, T.; Yamazaki, I. *Angew. Chem., Int. Ed.* **2001**, *40*, 3194–3198. (f) Choi, M.-S.; Aida, T.; Yamazaki, T.; Yamazaki, I. *Chem.—Eur. J.* **2002**, *8*, 2667–2678.

(10) Selected reviews on light-harvesting dendritic and hyperbranched polymers: (a) Bauer, R. E.; Grimsdale, A. C.; Müllen, K. *Top. Curr. Chem.* **2005**, *245*, 253–286. (b) Ceroni, P.; Bergamini, G.; Marchioni, F.; Balzani, V. *Prog. Polym. Sci.* **2005**, *30*, 453–473. (c) Jiang, D.-L.; Aida, T. *Prog. Polym. Sci.* **2005**, *30*, 403–422.

(11) Schlüter, A. D.; Wegner, G. *Acta Polym.* **1993**, *44*, 59–69.

(12) Banerjee, M.; Shukla, R.; Rathore, R. *J. Am. Chem. Soc.* **2009**, *131*, 1780–1786.

(13) (a) Weil, T.; Reuther, E.; Müllen, K. *Angew. Chem., Int. Ed.* **2002**, *41*, 1900–1904. (b) Metivier, R.; Kulzer, F.; Weil, T.; Müllen, K.; Basche, T. *J. Am. Chem. Soc.* **2004**, *126*, 14364–14365. (c) Berresheim, A. J.; Mueller, M.; Müllen, K. *Chem. Rev.* **1999**, *99*, 1747–1785.

Chart 1. (a) Structure Representation of PP-CMP and Coumarin 6 and (b) Schematic Representation of Energy Funneling from PP-CMP to Spatially Confined Coumarin 6[a]

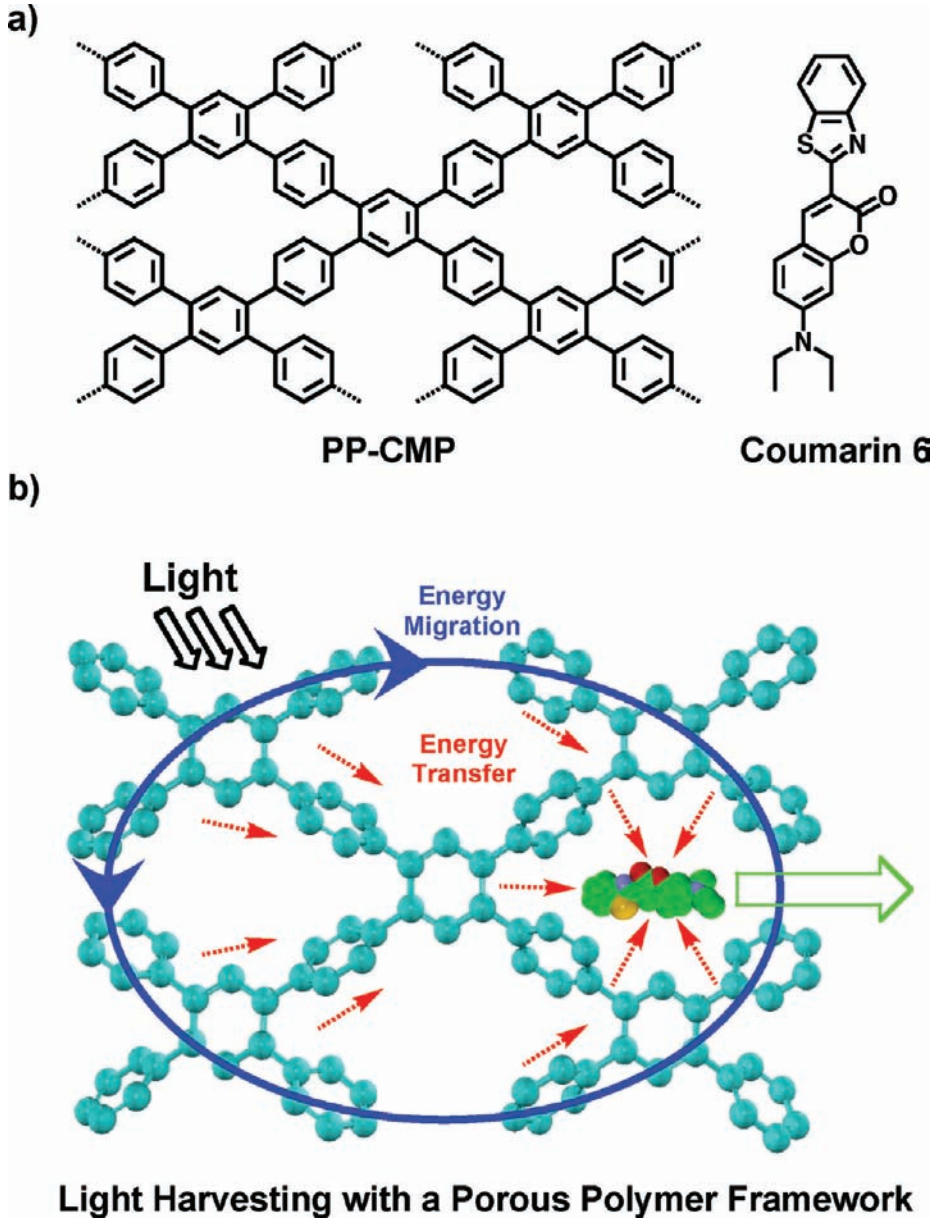

[a] Blue framework, PP-CMP; green framework, coumarin 6; H atoms are omitted.

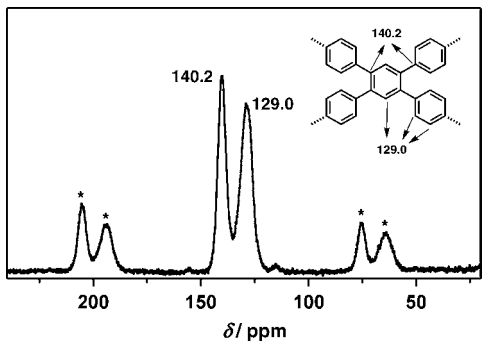

Figure 1. Solid-state $^{1}H-^{13}C$ CP/MAS NMR spectrum of PP-CMP, recorded at a MAS rate of 15k Hz and a CP contact time of 2 ms. Signals with * are sidebands.

and the resultant mixture was refluxed for 24 h. The precipitate was collected by centrifuge and washed with THF, acetone, and ethanol, to give a pale yellow solid in 88−93% yields. The content of coumarin 6 was evaluated by a standard curve method.[14] The synthesis of PP-CMP⊃coumarin 6 with different coumarin 6 contents, from 0.08 to 2.9 mol %, was successfully achieved by using different ratios of coumarin 6 to PP-CMP.

PP-CMP⊃coumarin 6 (content of coumarin 6 = 2.9 mol %) emitted green fluorescence at 512 nm, upon excitation of the PP-CMP framework at 363 nm (Figure 4c, solid red curve). Surprisingly, no fluorescence at 443 nm due to the PP-CMP framework was observed. These observations indicate that the

(14) (a) Inagaki, S.; Ohtani, O.; Goto, Y.; Okamoto, K.; Ikai, M.; Yamanaka, K.; Tani, T.; Okada, T *Angew. Chem., Int. Ed.* **2009**, *48*, 4042–4046. (b) Ramamurthy, V.; Shailaja, J.; Kaanumalle, L. S.; Sunoj, R. B.; Chandrasekhar, J. *Chem. Commun.* **2003**, 1987–1999.

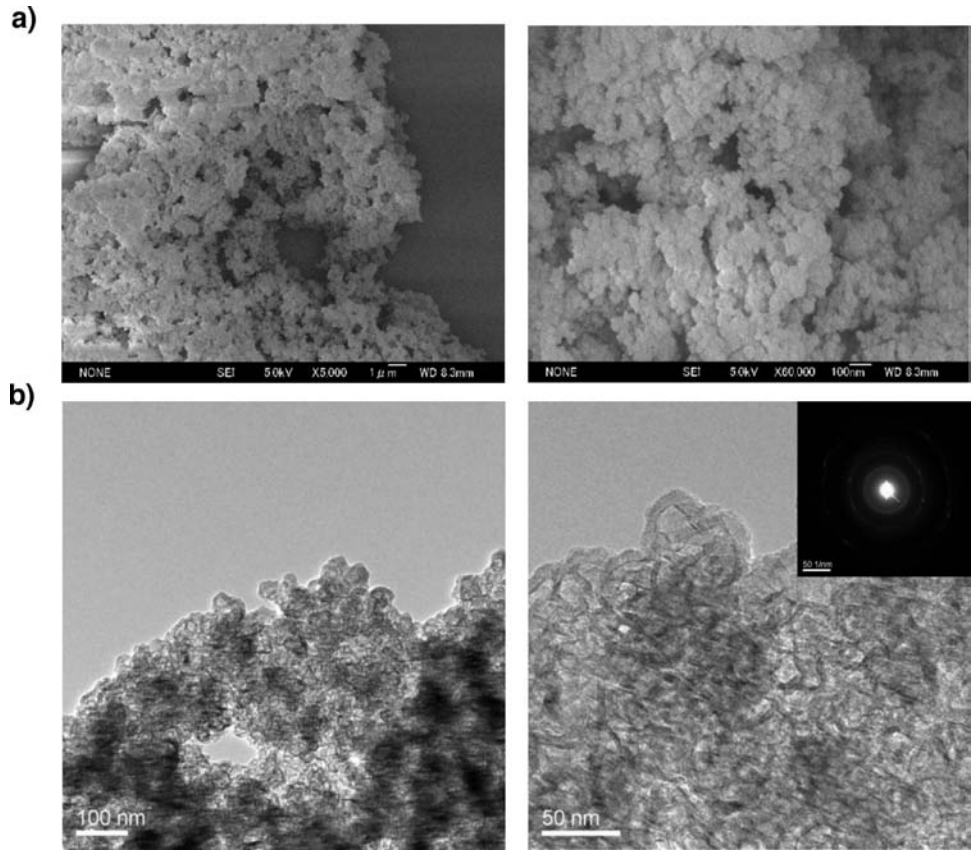

Figure 2. (a) FE SEM and (b) TEM images (Inset: SAED pattern) of PP-CMP.

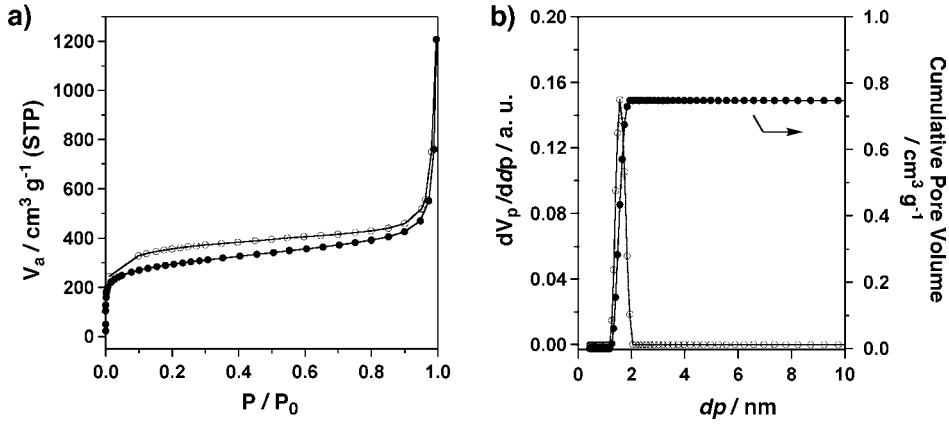

Figure 3. (a) N_2 sorption isotherm profile measured at 77 K and (b) pore width and distribution of PP-CMP.

excitation energy was transferred from the PP-CMP framework to coumarin 6. The excitation spectrum monitored at 512 nm resulted in a profile with maxima at 363 and 458 nm, assignable to the PP-CMP framework and coumarin 6, respectively (dotted red curve). The electronic absorption spectrum of PP-CMP⊃coumarin 6 does not show any sign of ground-state interaction between the PP-CMP framework and coumarin 6; therefore, comparison of the excitation spectrum with the absorption spectrum gave a quantum efficiency of energy transfer (Φ_{ENT}) as high as 91%. In sharp contrast, a solid mixture of PP-CMP with coumarin 6 under conditions otherwise identical to those described above does not show any fluorescence from coumarin 6 upon excitation of the PP-CMP framework, which indicates that no energy transfer occurs. The conjugated microporous polymer framework of PP-CMP⊃coumarin 6 serves as an energy funnel that harvests photons from the ultraviolet region and channels them to coumarin 6. The fluorescence intensity upon excitation of the PP-CMP framework is 21-fold as high as that of direct excitation of coumarin 6, due to the combination of the site isolation effect and the antenna effect (Figure S3). The fluorescence spectrum of coumarin 6 is highly sensitive to intermolecular interactions; therefore, it has been widely utilized as a probe for the detection of aggregation. For example, coumarin 6, when aggregated, emits an excimer-originated orange luminescence at 566 nm, while in the monomeric state, such as in dilute CH_2Cl_2 solution, it gives a green fluorescence at 497 nm (Figure 4b). Accordingly, the green emission with a band at 493−512 nm (see below) for PP-CMP⊃coumarin 6 suggests that the coumarin molecules are spatially isolated from one another and "independently" confined

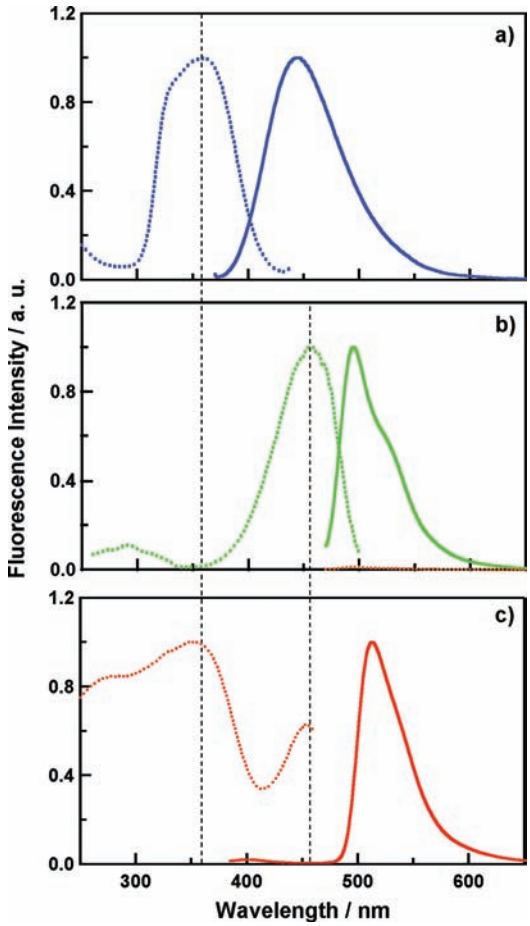

Figure 4. Normalized fluorescence excitation (dotted curve) and emission (solid curve) spectra of (a) PP-CMP (dotted blue curve monitored at 443 nm, solid blue curve upon excitation at 363 nm, dispersed in CH_2Cl_2/PEG), (b) coumarin 6 (dotted green curve monitored at 497 nm, solid green curve upon excitation at 458 nm, dotted orange curve upon excitation at 363 nm, in CH_2Cl_2), and (c) PP-CMP⊃coumarin 6 (content of coumarin 6 = 2.9 mol %; dotted red curve monitored at 512 nm, solid red curve upon excitation at 363 nm, dispersed in CH_2Cl_2/PEG).

in the microporous channel. This is further confirmed by the fact that the fluorescence quantum yield (60%) of coumarin 6 in PP-CMP⊃coumarin 6 is close to that for a dilute solution of coumarin 6 dissolved in CH_2Cl_2 (76%).

The luminescence of PP-CMP⊃coumarin 6 is highly dependent on the coumarin 6 content. As the content of coumarin 6 increased, the emission changed gradually from sky blue to brilliant green (Figure 5a). Quantitative evaluation using fluorescence spectroscopy showed that the intensity at 493−512 nm due to coumarin 6 increased while that from the PP-CMP framework decreased when the content of coumarin 6 was increased from 0 to 2.9 mol % (Figure 5b). Significantly, the relative fluorescence intensity $I_{\text{coumarin 6}}/I_{\text{PP-CMP}}$ (Figure S4) for PP-CMP⊃coumarin 6 (content of coumarin 6 = 2.9 mol %) is 40, which is approximately 200 times that of PP-CMP⊃coumarin 6 with a content of coumarin 6 = 0.08 mol % ($I_{\text{coumarin 6}}/I_{\text{PP-CMP}}$ = 0.2). This suggests that energy transfer from the PP-CMP framework to coumarin 6 is not a re-absorption of the fluorescence of the PP-CMP framework by coumarin 6. As a result, the Φ_{ENT} value increases with the coumarin 6 content in a sigmoidal fashion and levels off after 1.5 mol % (Figure 5c). Light-harvesting activity could be evaluated from the magnitude of the absorption cross-section and the efficiency of energy transfer. Thus, PP-CMP⊃coumarin 6 exhibits increased light-harvesting activity when the coumarin 6 content is increased; PP-CMP⊃coumarin 6 with the highest coumarin content of 2.9 mol % displays light-harvesting activity approximately 27 times that of PP-CMP⊃coumarin 6 with a low coumarin 6 content of 0.08 mol %. Along this line, we calculated how many phenyl units are effective in light-harvesting and energy-channeling. For PP-CMP⊃coumarin 6 with a coumarin 6 content of 2.9 mol %, approximately 176 phenylene units of the PP-CMP framework harvest the photons and funnel the excitation energy to one coumarin 6 molecule on average.

In the photochemical events in bacterial light-harvesting antenna complex LH2, the excitation energy is considered to be maintained in the wheel-like chromophore array without radiative decay, due to an excellent cooperativity among the chromophore units for energy migration. In order to evaluate the energy migration characteristics of PP-CMP⊃coumarin 6, steady-state fluorescence depolarization was investigated in a viscous medium of PEG at 25 °C, where molecular motions that lead to fluorescence depolarization should be suppressed.[15] The monomer mixture displayed a p value of about 0.32. In sharp contrast, PP-CMP had a low p value of 0.012 upon excitation at 363 nm, suggesting that the excitation energy is not localized but can migrate over the PP-CMP framework. On the other hand, excitation of PP-CMP⊃coumarin 6 (coumarin 6 content = 2.9 mol %) with a polarized light resulted in a highly depolarized fluorescence with an extremely low p value of only 0.02 at the emission band of 436 nm. In contrast, the p value for the encapsulated coumarin 6 was as high as 0.13.[16] These contrasting trends indicate the possible cooperation of subunits within the PP-CMP framework to facilitate energy migration. Such long-range excitation energy migration is quite interesting when considering the absence of any ordered alignment or orientation of subunits in the amorphous framework. Along this line, we further evaluated the intrinsic carrier mobility of PP-CMP by laser flash photolysis time-resolved microwave conductivity measurements (FP TRMC; see Supporting Information).[17a] The transient conductivity profile shows a rapid rise upon laser irradiation, yielding a $\Phi\Sigma\mu$ value of 6.1 $\times$ 10^{-6} cm^2 V^{-1} s^{-1} at a photon density of 3.12 $\times$ 10^{16} photons cm^{-2} (Figure 6a). To evaluate the exciton−exciton annihilation effect on the carrier generation, experiments with lasers at different photon densities and different wavelengths were carried out (Figures S5−7). It is noticed that the $\Phi\Sigma\mu$ values are almost constant with 355 nm laser irradiation at photon densities ranging from 1.4 $\times$ 10^{16} to 3.8 $\times$ 10^{16} photons cm^{-2} (Figure

(15) Here, fluorescence anisotropy (p) is defined by $(I_{\parallel} - GI_{\perp})/(I_{\parallel} + GI_{\perp})$, where $I_{\parallel}$ and $I_{\perp}$ are fluorescence intensities of parallel and perpendicular components relative to the polarity of the excitation light, respectively, and G is an instrumental correction factor.

(16) Because PEG hardly enters into the 3D pores of PP-CMP, the relatively low p value (p = 0.13) observed for coumarin 6 in PP-CMP⊃coumarin 6 (dispersed in PEG/CH_2Cl_2) in comparison with that in PEG/CH_2Cl_2 (p = 0.31) may suggest that coumarin 6 in the pores of PP-CMP (probably CH_2Cl_2 enters into the pores) has a relatively high mobility compared with that fixed in the highly viscous PEG media.

(17) (a) Santoro, A. V.; Mickevicius, G. *Chem. Phys. Lett.* **1975**, *36*, 658–660. (b) Vaughan, G. B. M.; Heiney, P. A.; McCauley, J. P., Jr.; Smith, A. B. *Phys. Rev. B* **1992**, *46*, 2787–2791. (c) Acharya, A.; Seki, S.; Koizumi, Y.; Saeki, A.; Tagawa, S. *J. Phys. Chem. B* **2005**, *109*, 20174–20179. (d) Yamagami, R.; Kobayashi, K.; Saeki, A.; Seki, S.; Tagawa, S. *J. Am. Chem. Soc.* **2006**, *128*, 2212–2213. (e) Dicker, G.; de Haas, M. P.; Warman, J. M.; de Leeuw, D. M.; Siebbeles, L. D. A. *J. Phys. Chem. B* **2004**, *108*, 17818–17824. (f) Dicker, G.; de Haas, M. P.; Siebbeles, L. D. A.; Warman, J. M. *Phys. Rev. B.* **2004**, *70*, 045203. (g) Li, W.-S.; Yamamoto, Y.; Fukushima, T.; Saeki, A.; Seki, S.; Tagawa, S.; Masunaga, H.; Sasaki, S.; Takata, M.; Aida, T. *J. Am. Chem. Soc.* **2008**, *130*, 8886–8887.

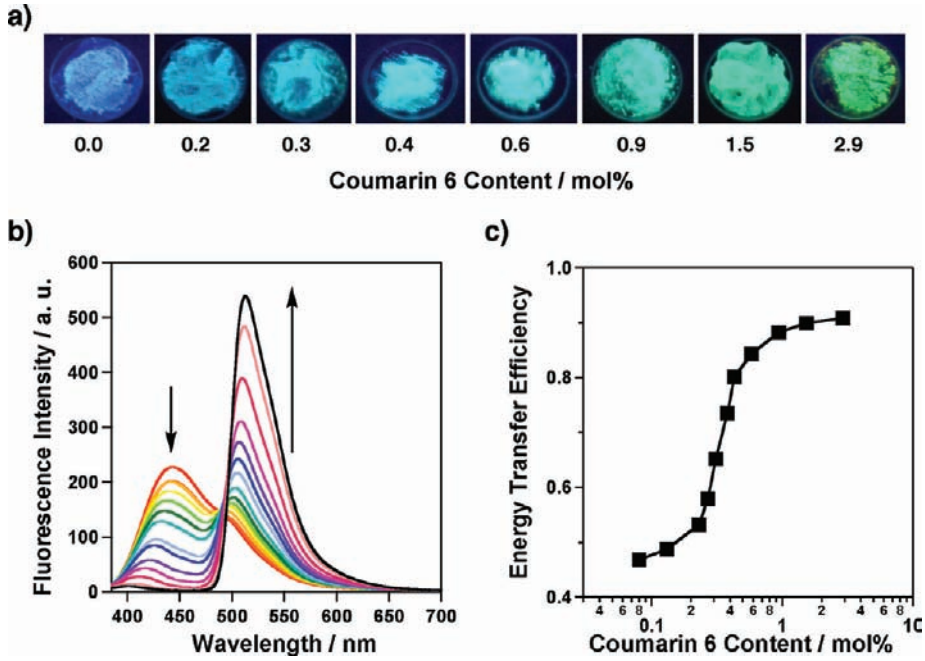

Figure 5. (a) Fluorescence images of solid samples of PP-CMP⊃coumarin 6 upon excitation at 363 nm. (b) Fluorescence spectral change of PP-CMP⊃coumarin 6 with different coumarin 6 contents upon excitation at 363 nm. (c) Plot of quantum efficiency of energy transfer from PP-CMP to coumarin 6 versus coumarin 6 content.

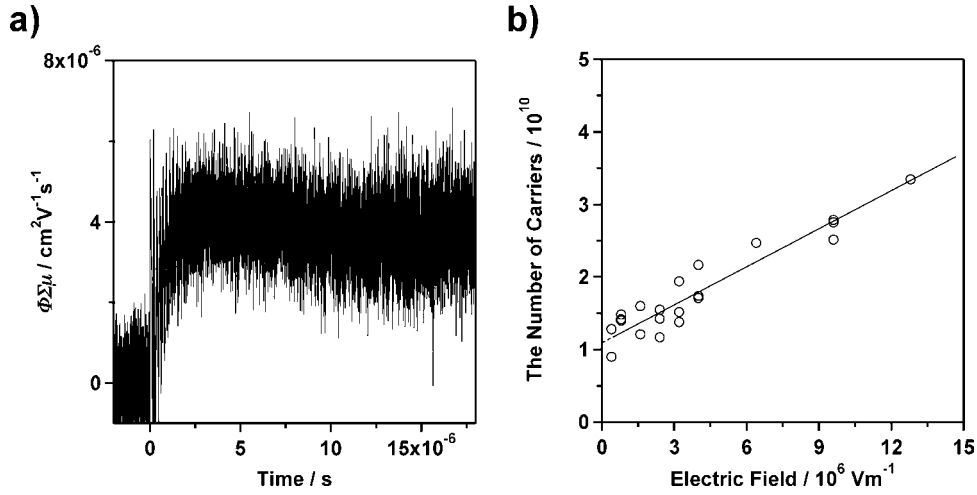

Figure 6. (a) FP TRMC profile of PP-CMP at 25 °C and (b) dependence of the number of charge carriers of PP-CMP on electric field density upon irradiation with a 355 nm pulse laser at a power of 3.12×10^{16} photons cm^{-2} (irradiation area = 1.9×10^{-3} cm^2).

S5b−-f), which suggests that the free charge carriers are generated by single-photon processes via the PP-CMP excited states.[18] To determine the number of charge carriers, time-of-flight transient was integrated at different electric fields (Figures 6b, Figure S7). The number of charge carriers estimated by extrapolation of the electric field at 0 V cm^{-1} was 1.14×10^{10}, leading to a charge carrier generation yield (Φ, number of charge carrier/number of photon) of 1.9×10^{-4}. Therefore, the minimum carrier mobility ($\Sigma\mu$) was evaluated to be 0.04 cm^2 V^{-1} s^{-1}. The intrinsic carrier mobility is higher than those of small organic semiconductors,[17b] one-dimensional conjugated polymers[17c] including the state-of-the-art semiconducting polymer RR-P3HT (μ = 0.014 cm^2 V^{-1} s^{-1}),[17d−f] and liquid crystalline systems.[17g]

To gain insight into the energy-transfer process, we carried out time-resolved fluorescence spectroscopy of thin films of PP-CMP and PP-CMP⊃coumarin 6 (content of coumarin 6 = 2.9 mol %) upon excitation of PP-CMP skeletons at 355 nm with a Nd:YAG laser. At 0 ns after laser pulse exposure, a major transient fluorescence peak due to coumarin 6 appeared at 499 nm, together with a relatively small emission at 443 nm from the PP-CMP framework (Figure 7a, red curve). At 1 ns, the emission from the PP-CMP framework decreased, while that of coumarin 6 increased (Figure 7a, black curve). At 3 ns, the emission of the PP-CMP framework further decreased, resulting in an almost pure emission from coumarin 6. Such a development of time-dependent transient fluorescence clearly indicates

(18) (a) Dicker, G.; de Hass, M. P.; Siebbeles, L. D. A. *Phys. Rev. B* **2005**, *71*, 155204. (b) Piris, J.; Dykstra, T. E.; Bakulin, A. A.; van Loosdrecht, P. H. M.; Knulst, W.; Trinh, M. T.; Schins, J. M.; Siebbeles, L. D. A. *J. Phys. Chem. C* **2009**, *113*, 14500–14506. (c) Siebbeles, L. D. A.; Huijser, A.; Savenije, T. J. *J. Mater. Chem.* **2009**, *19*, 6067–6072.

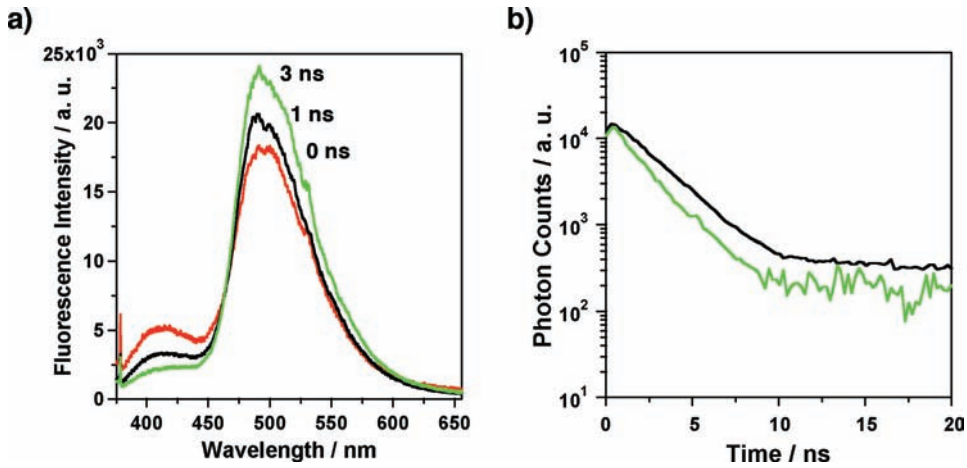

Figure 7. (a) Transient fluorescence spectra of PP-CMP⊃coumarin 6 (coumarin 6 content = 2.9 mol %) observed at 0, 1, and 3 ns after exposure to laser pulse. (b) Fluorescence decay profiles of PP-CMP (black curve) and PP-CMP⊃coumarin 6 (green curve, coumarin 6 content = 2.9 mol %) observed for the fluorescence in the 410−425 nm range.

that the time scale required for the energy transfer is on the nanosecond level. To evaluate the rate constant of energy transfer, we measured the lifetime of fluorescence at 410−425 nm due to the PP-CMP framework. The PP-CMP film exhibited a pseudo-single-component decay profile, with an average lifetime (τ_0) of approximately 2.6 ns (Figure 7b, black curve). On the other hand, the lifetime (τ_{DA}) of PP-CMP⊃coumarin 6 was significantly decreased to be only 1.8 ns (Figure 7b, green curve). Accordingly, the pseudo-first-order rate constant of the energy transfer from PP-CMP to coumarin 6 in the film was estimated to be as high as 1.7×10^8 s^{-1} using the equation ${\tau_0}^{-1} - {\tau_{DA}}^{-1}$, which leads to a value of 1.2×10^{10} M^{-1} s^{-1} when taking the concentration of coumarin 6 into account. These results suggest that the energy-transfer process is controlled by rapid exciton diffusion, and such a speedy energy transduction is unprecedented for conjugated microporous polymers and rare for other polymeric light-harvesting antennae.

Conclusions

Exploration of conjugated microporous polymers has a high probability of leading to the development of new materials. In summary, we found an unprecedented light-harvesting CMP by designing energy-donating polyphenylene skeletons as antenna in conjunction with the exploration of the inherent micropores for the spatial confinement of energy-accepting coumarin 6 molecules. PP-CMP is capable of excitation energy migration over the conjugated framework and allows for rapid carrier transportation with large mobility. PP-CMP enables high-throughput noncovalent synthesis of PP-CMP⊃coumarin 6 with tunable donor−acceptor compositions. Moreover, PP-CMP⊃coumarin 6 harvests a wide range of photons from the ultraviolet to visible regions and converts them to brilliant green luminescence. PP-CMP skeletons trigger rapid, vectorial, and highly efficient energy channeling to the acceptors. These characteristics are unique and clearly originate from the conjugated porous structures. Therefore, the light-harvesting antennae constitute an important step for molecular optoelectronics based on porous polymeric materials.

Acknowledgment. This work was supported by Precursory Research for Embryonic Science and Technology (PRESTO), Japan Science and Technology Agency (JST) (D.J.). D.J. thanks the JSPS Asian core program.

Supporting Information Available: Details regarding the synthetic procedure, full methods, FT-IR and fluorescence spectra, and PXRD profile. This information is available free of charge via the Internet at http://pubs.acs.org.

JA100327H